Predicting Shrinkage and Porosity of Cotton and Hemp Fabrics Using FIG-PSO-ELM Algorithm

Xia Hou
School of New Materials and Shoes & Clothing Engineering, Liming Vocational University, Quanzhou, 362000, China
E-mail: houxia20222022@163.com

Keywords: FIG-PSO-ELM, cotton and linen fabric, polycondensation performance, bulkiness

Received: June 25, 2024

Cotton and linen fabric is a mixed textile of half linen and half cotton, which has the characteristics of both linen and cotton, so it is widely used in summer clothes. Shrinkage and bulk properties are important indicators of the quality of cotton and linen fabrics, so it is necessary to predict their shrinkage and bulk properties accurately. The extreme learning machine algorithm is introduced to predict the fluctuation range, and the particle swarm optimization algorithm is used to optimize it. Furthermore, fuzzy information granulation (FIG) technology is employed to achieve the dynamic extraction of characteristics associated with cotton-hemp blended fabrics. This is achieved through the construction of an FIG-PSO-ELM algorithm, the efficacy of which is subsequently verified. The experimental results showed that the shrinkage rate and elastic viscosity of cotton and linen blended fabric changed significantly within 1500 seconds. The value range was 49.2 to 51.2, and the maximum value was 51.15. In addition, the prediction results of the FIG-PSO-ELM method in the minimum value (Low), the average value (R), and maximum value (Up) sequences were consistent with the actual values, showing good prediction accuracy. Compared with the prediction results of the other four algorithms, such as BPNN, RBFNN, PSO-ELM, and traditional ELM, FIG-PSO-ELM had the smallest errors on the three sequences, with the lowest values of 0.0019 and 0.0368, respectively. Overall, the FIG-PSO-ELM method has a good prediction effect, accurately predicts the polycondensation area and porosity of cotton and linen fabrics, and has a good effect on the actual weaving of cotton and linen fabrics.

Povzetek: Razvit je nov napovedni model FIG-PSO-ELM za natančno napovedovanje krčenja in poroznosti bombažnih in lanenih tkanin.

1 Introduction

Cotton and linen fabrics are widely used in textile materials for summer clothing because of their natural environmental protection and good air permeability. Cotton and linen fabrics combine the strength of linen with the softness of cotton, complementing each other's advantages and disadvantages, making them excellent materials for textiles [1]. In cotton and linen fabrics, the two characteristics of shrinkage and porosity are important indicators to test their quality. Predicting the fluctuation of the two indicators is an important way to improve cotton and linen fabrics [2]. Domestic scholars have conducted in-depth research on this basis. Saricam C believed that the thermal conductivity, fiber, and shrinkage properties of blended fabrics such as cotton and linen helped to improve their comfort [3]. Nongnual et al. proposed a drop shape analysis method using a computer algorithm for image brightness detection, thereby realizing the precise estimation of the sliding angle and providing a new idea for the commercial use of cotton and linen fabrics [4]. Birkocak compared the porosity of different fabrics such as cotton and flax fibers and found that it helps to improve the quality and strength of cotton and linen fabrics [5]. However, there is currently almost no data-driven modeling research on the performance of cotton and linen fabrics, and there is no effective method for predicting the porosity characteristics of cotton and linen fabrics. Therefore, the study introduces an Extreme Learning Machine (ELM), and uses the Particle Swarm Optimization (PSO) algorithm to make the optimization in practical applications. It also introduces Fuzzy Information Granulation (FIG) technology, which constitutes the FIG-PSO-ELM algorithm. The purpose is to realize the effective prediction of the fluctuation range of the shrinkage and looseness characteristics of cotton and linen fabrics to improve its quality.

2 Related work

Fabric is one of the three elements of clothing, that affects the style and characteristics of clothing, as well as the color and shape of clothing [6]. In fabric quality and strength, polycondensation performance and porosity occupy a certain proportion. Therefore, accurately predicting the fluctuation range of the two in the process

of fabric production is helpful to improve its quality [7]. Based on this, scholars around the world have tried to study it in detail. Zhang et al. proposed a more environmentally friendly enzymatic method to improve the shrink resistance of wool fabrics and effectively improve their polycondensation performance [8]. Luo et al. developed a new continuous pad dyeing method, which effectively reduced the shrinkage of wool fabrics and improved their color fastness [9]. Liu et al. synthesized a new N-phenyl maleimide, which effectively improved the polycondensation performance and comfort of wool fabrics and enhanced their antibacterial properties [10]. Šaravanja et al. studied the effects of dry and wet cleaning on three types of fabrics, which helped to improve fabric strength and shrinkage properties [11]. Qi et al. used a two-step method to develop a cotton fabric with different heat transfer properties. While the shrinkage performance of the cotton fabric was improved, its thermal insulation effect was also effectively enhanced [12]. Fahritdinovna et al. provided constructive suggestions for improving the quality of national fabrics through an in-depth study of the fiber composition of garment fabrics [13].

In addition, Zhang et al. realized the adjustable porosity of medical protective garments, which is conducive to improving their tensile strength [14]. Fouda et al. studied the thermophysical properties of single jersey knitted fabrics to improve their wear resistance and air permeability [15]. Dehghan et al. analyzed the thermal properties of textiles to determine the effect of porosity, etc., which effectively helped to improve their quality [16]. Kim et al. studied the changes in the internal structure of silk gauze under different hot-pressing times, which helped to improve its elongation and reduce its porosity [17]. Kim and Um analyzed the effect of pressing temperature on the porosity of the fabric in detail, thus assisting in the production of silk non-woven fabrics with more properties [18]. The above contents are summarized in Table 1.

Table 1: Summary of references

Reference number	Author	Research Outcome Description	Potential Shortcomings
[8]	Zhang et al	Develops an eco-friendly enzymatic method to enhance wool fabric shrink resistance and shrinkage performance.	Scale and economic analysis is required.
[9]	Luo et al	Introduces a new continuous pad dyeing method to reduce wool fabric shrinkage and improve color fastness.	Long-term fabric performance data are limited.
[10]	Liu et al	Utilizes a novel N-phenylmaleimide to improve wool fabric properties.	Need to increase durability research.
[11]	Šaravanja et al	Examines the effects of dry and wet cleaning on fabric properties.	Limited universality across fabric types.
[12]	Qi et al	Develops cotton fabric with improved thermal properties using a two-step method.	Applicability to other fabric types is not discussed.
[13]	Fahritdinovna et al	Studies fiber composition to improve ethnic fabric quality.	A thorough analysis of all relevant fibre properties is required.
[14]	Zhang et al	Uses coating technology to adjust porosity in medical protective clothing.	Assessment of comfort and breathability is not mentioned.
[15]	Fouda et al	Investigates the thermo-physiological properties of knitted fabrics.	Applicability to different knitting techniques is unknown.
[16]	Dehghan et al	Analyzes the thermal properties of textiles to determine the role of porosity.	Variability under different environmental conditions is not addressed.
[17]	Kim et al	Studies the effect of hot press cycles on silk non-woven fabric structure.	The effect of different pressure temperatures on fabric structure is not specified.
[18]	Kim and Um	Analyzes the effect of pressing temperature on silk non-woven fabric porosity.	Different press times and their effects are not discussed.

A review of the literature reveals a dearth of data-driven modeling studies on the properties of cotton and linen fabrics. Furthermore, there is currently no method for predicting the porosity characteristics of these fabrics that is both relatively effective and widely applicable. Therefore, the study proposes the FIG-PSO-ELM method. The FIG-PSO-ELM method is proposed out of the need for accurate prediction of the

polycondensation properties and porosity of cotton and linen fabrics, which is crucial to ensure product quality and production efficiency. Existing studies lack effective data-driven models to dynamically predict these characteristics, but FIG-PSO-ELM provides an innovative solution by combining FIG technology to process dynamic data and using PSO algorithm to improve the prediction accuracy of ELM.

3 The shrinkage performance and porosity of cotton and linen fabrics based on the ELM algorithm

3.1 ELM Algorithm for Data-Driven Modeling

To improve the polycondensation performance and porosity of cotton and linen fabrics, ELM is used to predict the range of variation of polycondensation performance and porosity of cotton and linen fabrics, and the effectiveness of the design is verified. As a new type of feed-forward neural network with a single hidden layer, ELM has the corresponding weights of randomly generated input layers and the relevant thresholds of hidden layers. ELM does not need to make any adjustments. Only by setting the number of neurons in the hidden layer, the optimal solution can be obtained by using the least square method. Compared with the traditional neural network, ELM solves the problem of inefficiency and complex parameter updating caused by the back-propagation algorithm, and also simplifies the network parameter setting, fast training, and generalization performance [19]. The simplest three-layer ELM network structure is shown in Figure 1.

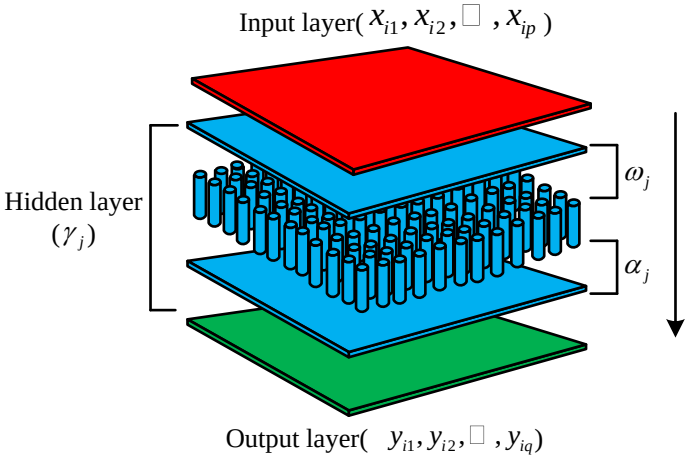

Figure 1: Schematic diagram of three-layer ELM network structure

From Figure 1, the three-layer ELM includes an input layer, a hidden layer, and an output layer, and the activation function selected inside must be infinitely differentiable in any range. Among them, e represents the maximum number of particles in the input layer. q represents the maximum number of particles in the output layer. In addition, the corresponding expression of ELM output in hidden layer neurons is expressed in formula (1).

$$f\left(x_i\right)=\sum_{j=1}^{L}\alpha_j g\left(\omega_j x_i+\gamma_j\right) \tag{1}$$

In formula (1), $f\left(x_i\right)$ represents the output value of the hidden layer ELM. L represents the number of neurons in the hidden layer. j represents the j-th neuron. i represents the number of training samples. α_j represents the connection weight between the hidden layer neurons and the output layer. $g(\cdot)$ is the activation function of the hidden layer. ω_j represents the weight of the input layer. x_i represents the input value of the input layer. γ_j represents the threshold of the hidden layer neurons. The purpose of ELM learning is to minimize the output error, so its expression is formula (2).

$$\sum_{i=1}^{M}\left\| f\left(x_i\right)-y_i\right\|=0 \tag{2}$$

In formula (2), M represents the maximum number of training samples. y_i represents the output value of the output layer. According to formula (2), there is an equation between the weights of the two sections, the weights of the input layer, and the output of the output layer. Its expression is shown in formula (3).

$$\sum_{j=1}^{L}\alpha_j g\left(\omega_j x_i+\gamma_j\right)=y_i \tag{3}$$

According to formula (3), the matrix expression can be introduced to simplify it accordingly. Its simplified expression is shown in formula (4).

$$\begin{cases} H\alpha = Y \\ H = \begin{bmatrix} g(\omega_1 x_1 + \gamma_1) & \text{L} & g(\omega_L x_1 + \gamma_L) \\ \text{M} & & \text{M} \\ g(\omega_1 x_M + \gamma_1) & \text{L} & g(\omega_L x_M + \gamma_L) \end{bmatrix} \in R^M \times R^L \end{cases} \quad (4)$$

In formula (4), H represents the output matrix of the hidden layer. α represents the output weight matrix of the hidden layer. Y represents the expected output matrix. R represents the overall matrix. Since the input layer weights and hidden layer thresholds of H ELM are random, they can be regarded as a known output matrix. On this basis, according to the value α that can be obtained by the least square method, its evaluation formula is shown in formula (5).

$$\hat{\alpha} = H^{+}Y \quad (5)$$

In formula (5), H^{+} represents the narrow sense inverse matrix. According to the derivation process of formula (1) to formula (5), the training process of the H ELM algorithm can be given. Its training process is shown in Figure 2.

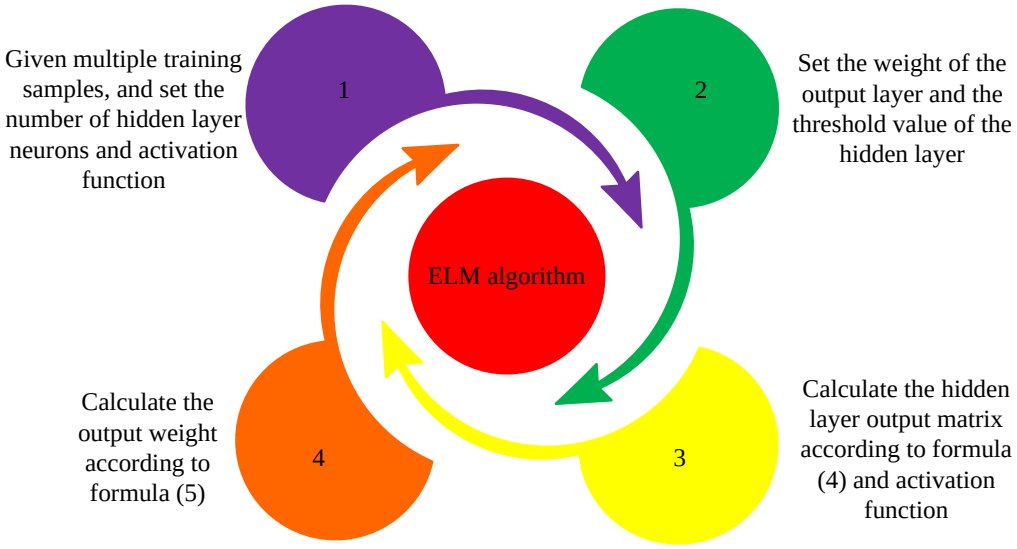

Figure 2: ELM algorithm training process

From Figure 2, the training process of the ELM algorithm first gives multiple training samples, and sets the number of hidden layer neurons and activation functions. Second, it uses the random principle to set the weights and hidden layers of the output layer and the layer threshold. Then, it calculates the output hidden layer matrix according to formula (4) and the given activation function. Finally, the output weight is calculated according to formula (5), and the model obtained at this time is trained and can be directly used to predict the test samples. After the ELM training process, it can be known that the ELM is derived from a single hidden forward neural network, which also has the nonlinearity of the neural network. Compared with the traditional neural network, ELM only needs to set the number of neurons in the hidden layer in the initial stage, which reduces the cost of learning time and improves the versatility of the network. Therefore, in this study, ELM is selected as the basic algorithm to predict and model the shrinkage and porosity of cotton and linen fabrics.

3.2 PSO-ELM algorithm and FIG technology

In the actual production process of cotton and linen fabrics, dynamic data is used much more frequently than static data, and the data in the database is stored fluidly, that is, the data is generated sequentially. However, when training the ELM algorithm, all training samples are used to compute the output matrix. If the training samples are dynamic, the ELM algorithm will train every time a new training sample arrives until all new samples have arrived and no new samples have been generated. This will consume a lot of time. In addition, the polycondensation process of cotton and linen fabrics has the characteristics of high nonlinearity and complexity, so it is necessary to improve the traditional ELM to strengthen the stability of the prediction model. The PSO algorithm is a method based on swarm intelligence to achieve the optimal goal through optimal particle accumulation and optimal tracking [20]. During the iterative process of the PSO algorithm, the velocity and position need to be updated. Its velocity and position updating formulas are shown in formulas (6) and (7).

$$v_{od}^{t+1} = \omega' v_{od}^{t} + c_1 r_1 \left(p_{od} - x_{od}^{t} \right) + c_2 r_2 \left(p_{bd} - x_{od}^{t} \right) \quad (6)$$

Formula (6) is the particle velocity update formula. Among them, v_{od}^{t+1} represents the updated particle speed. v_{od}^{t} represents the particle speed before the update. ω' is the inertia weight, which can adjust the searchability of the particle. ω' represents the current iteration number. p_{od} is the extreme value of the particle individual. p_{bd} represents the group extreme value of the particle swarm. c is the learning factor, which can adjust the flight step. r is a random number, whose value is maintained between [0, 1]. d represents the dimension of the particle.

$$x_{od}^{t+1} = x_{od}^{t} + v_{od}^{t+1} \quad (7)$$

Formula (7) is the particle position update formula. x_{od}^{t+1} represents the updated particle position. In addition, the expressions of individual extremum and group extremum of particles in formula (6) are shown in formula (8) and formula (9).

$$p_o = \left(p_{o1}, p_{o2}, \mathrm{L}\ , p_{oD} \right) \quad (8)$$

In formula (8), o represents the serial number of the particle in the individual extremum. D is the maximum value of the particle dimension.

$$p_b = \left(p_{b1}, p_{b2}, \mathrm{L}\ , p_{bD} \right) \quad (9)$$

In formula (9), b is the serial number of the particle in the population extremum. From the principle of PSO algorithm and formula (6) to formula (9), PSO has the advantages of fast convergence, fewer parameters and simple and easy implementation. Therefore, the study combines the PSO with ELM to obtain the PSO-ELM, which effectively improves the efficiency. The training steps of PSO-ELM are shown in Figure 3.

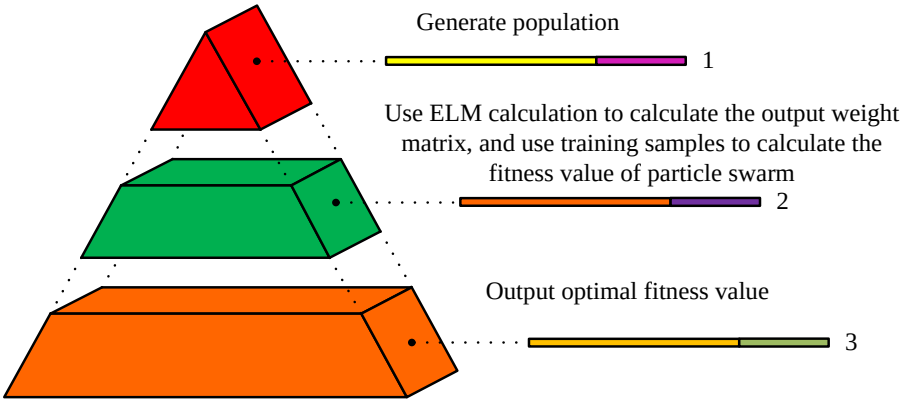

Figure 3: PSO-ELM training steps

From Figure 3, the training steps of the PSO-ELM algorithm network can be roughly divided into three steps. First, the population is generated. For complex problems, the number of particles can be set to 100-200. The particles in the population consist of an input weight matrix and a hidden layer offset. Second, the ELM algorithm is used to compute the corresponding weight matrix, and the training samples are used to compute the root mean square error of each particle to compute the fitness value of the PSO-ELM algorithm. Finally, the optimal fitness value is output. In addition, the research also uses FIG technology to extract the characteristics of the time series of fabric shrinkage. Information granulation is first proposed by Professor LAZ adeh in the United States. It essentially decomposes the similarity of elements in the set into a series of subsets, and each subset is a particle of information. There are three basic theories in the information granulation model, among which the fuzzy set theory is chosen in the research. The reason is that the fuzzy set theory can better describe incomplete knowledge. The expression of FIG technology, which is constructed based on information granulation and fuzzy set theory, is shown in formula (10).

$$a = \left(z \quad is \quad A \right) \quad is \quad \lambda \quad (10)$$

In formula (10), A represents the fuzzy subset. z represents the variable in the domain of discourse. λ represents the probability that the variable falls in the fuzzy subset. In a given time series, the granulation process of fuzzy information is mainly divided into two stages, which are window segmentation and fuzzy processing. Window segmentation is to divide the time series into several small sequences at equal intervals, and each small sequence is an operation window. Fuzzification is to establish a fuzzy particle in each operation window, that is, a fuzzy subset that can express variables reasonably. In formula (10), the task of fuzzification is to determine the membership function of the fuzzy subset. Generally, in the process of granulation, the shape of fuzzy particles must be determined first, and

then their degree of membership can be determined. The study uses a triangular blur particle. The membership function expression of this particle is shown in formula (11).

$$W(z,a,m,n,r)=\begin{cases}0, x<a\\ \dfrac{z-a}{m-a}, a\le z\le m\\ \dfrac{r-z}{r-n}, n\le z\le r\\ 0, z>r\end{cases} \tag{11}$$

In formula (11), a, m and r are the parameters of the fuzzy subset, which correspond to the minimum value (Low), the average value (R), and maximum value (Up) of the operation window, respectively. W represent the membership function of the fuzzy subset. The specific steps of the granulation method used in the study are shown in Figure 4.

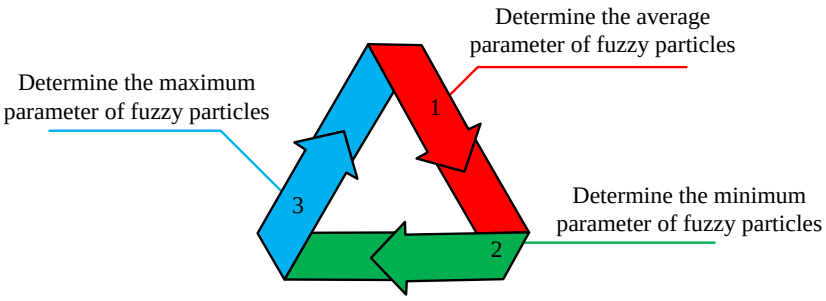

Figure 4: Specific steps of the granulation method used in the study

From Figure 4, the granulation method first determines the average parameter of fuzzy particles, then determines the minimum parameter of fuzzy particles, and finally determines the maximum parameter of fuzzy particles. When determining the Low value of fuzzy particles, the corresponding calculation formula is shown in formula (12).

$$MinimizeQ(a)=\frac{\sum_{x_k'\le\left\lfloor\frac{N}{2}\right\rfloor}W(x_k')}{m-a} \tag{12}$$

In formula (12), x' represents the element in the time series, and the maximum value is x_N'. $\lfloor\ \rfloor$ represents the sign of rounding down. In addition, when determining the Up value of fuzzy particles, the corresponding calculation formula is shown in formula (13).

$$MaximizeQ(r)=\frac{\sum_{x_k'\ge\left\lceil\frac{N}{2}\right\rceil}W(x_k')}{r-m} \tag{13}$$

In formula (13), $\lceil\ \rceil$ is the sign of rounding up. In data preprocessing, FIG technology is mainly used for in-depth data analysis. In data-driven model research, FIG and machine learning are generally combined to perform step-by-step interval prediction based on the original point prediction. FIG technology is excellent in feature extraction and can realize effective interval prediction, so it is used in research to predict the shrinkage performance of cotton and linen fabrics and the fluctuation range of porosity.

3.3 Prediction of polycondensation performance and porosity fluctuation range of cotton and linen fabrics based on FIG-PSO-ELM

In the prediction of the fluctuation range, the research combines FIG technology with PSO-ELM to obtain the FIG-PSO-ELM algorithm. Its core firstly combines the obtained three characteristic components, namely the maximum, average and minimum three characteristic components, in a certain period, which reflects the fluctuation range of shrinkage performance. Secondly, since it is static to use the past amplitude to predict the future amplitude, the combination of FIG and PSO-ELM algorithms can effectively predict the characteristic components. The variations in shrinkage and porosity of cotton and linen fabrics will have a certain impact on the subsequent textile relief. Therefore, it is necessary to abandon the traditional idea of point prediction and expand to the prediction of its fluctuation range. The shrinkage performance of cotton and linen fabrics refers to the use of a fixed clip to secure the two ends of the fabric under standard atmospheric pressure. Under the action of external force, one end of the fabric gradually shrinks toward the other end. When the fabric is gathered

to the maximum without wrinkles, the ratio of the length of the fiber after movement to the original length of the fabric is the final shrinkage rate [21]. Bulkiness refers to the ratio of the length of movement of a fabric to the original length of the fibers, where one end of the fabric is held together by external force and the other end shrinks inward without wrinkling [22]. Based on this, the research builds the FIG-PSO-ELM algorithm model, and its process is shown in Figure 5.

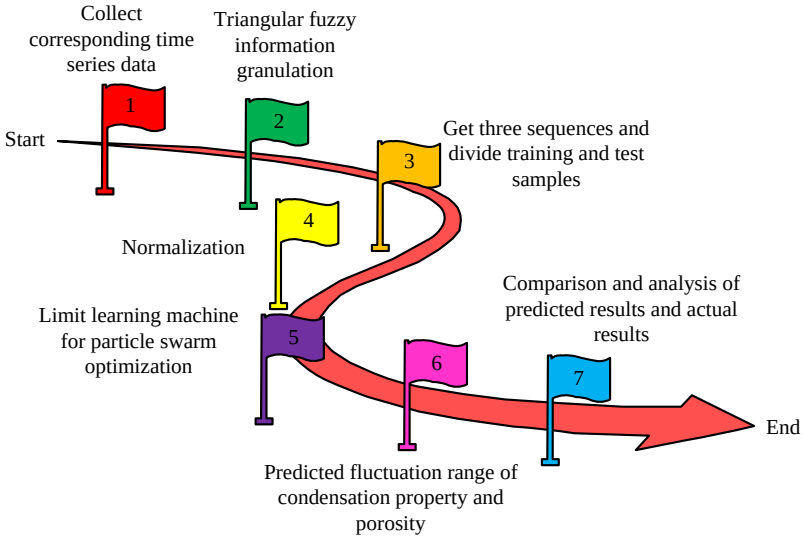

Figure 5: FIG-PSO-ELM algorithm model flow diagram

From Figure 5, the FIG-PSO-ELM process is mainly divided into two stages: offline training and online prediction. In the offline training stage, firstly, the original time series-related data of cotton and linen fabric shrinkage and porosity are used as samples. Secondly, the size of the corresponding window is divided, and the sample is fuzzy information granulated using the formula (11). Then the step size is determined and the first three quarters of the data of each sequence are set as training samples and the remaining data as test samples. Next, the three sequences of Low, R, and Up are normalized and processed to [0, 1]. After the normalization process is completed, the three sequences in the training samples can be input into the ELM for corresponding training. Finally, the average deviation is used as the adaptive degree function based on the training samples, and the PSO is utilized to optimize the weight of the ELM and the hidden layer threshold. In the online test phase, first, the three sequences in the test sample are input into the ELM model trained in the offline phase for the corresponding prediction. Second, the predicted results are compared with the actual results. When the offline training is used to normalize the three-sequence data, the corresponding normalization formula is shown in formula (14).

$$x_i'' = \frac{x_i - x_{\min}}{x_{\max} - x_{\min}} \tag{14}$$

In formula (14), x'' is the normalized data. x_i represents the data of a certain attribute in the training sample. $x_{\min}$ and $x_{\max}$ are the minimum and maximum values of the column data corresponding to the attribute. In addition, before the experiment, it is necessary to set the corresponding performance index. The study uses the mean square error and means absolute error of the test sample as the evaluation index to analyze the prediction error accordingly. The corresponding calculation formula is shown in formula (15).

$$\begin{cases} MSE = \dfrac{1}{D}\sum_{i=1}^{D}\left(\beta_i - \beta_i'\right) \\ MAE = \dfrac{1}{D}\sum_{i=1}^{D}\left|\left(\beta_i - \beta_i'\right)\right| \end{cases} \tag{15}$$

In formula (15), MSE represents the mean square error. D represents the number of test samples. β_i represents the actual value of the test sample. β_i' is the predicted value of the test sample. MAE represents the mean absolute error.

4 Performance analysis of FLG-PSO-ELM in practical applications

To verify the effectiveness of the FLG-PSO-ELM algorithm in predicting the shrinkage performance and porosity fluctuation range of cotton and linen fabrics, the research carried out corresponding simulation training. Before the experiment, the research set up the experimental data according to the corresponding experimental conditions (the main data resources came

from a company's distributed control system). The content is shown in Table 2.

Table 2: Pre-setting content of experimental data

Number of original sequence data	Time between windows	Number of windows	Input value in the next window	Time (Coagulation performance characteristics)
1440	5min	288	First four windows	First 20 minutes
Time (Characteristic fluctuation range)	Number of samples	Training sample data	Test sample data	Operating environment
5 minutes after	284	Top 3/4	Rear 1/4	MATLAB R2017a

From Table 2, the study takes one minute as the sampling period to analyze the characteristics of shrinkage and bulkiness of 1440 cotton and linen fabrics. In a 5 -minute window, the fuzzy information of the original time series data is granulated, and a total of 288 windows are set. The values of the first 4 windows are used as input to predict the next window. In the first 20 minutes, the eigenvalues are used to predict the range of characteristic fluctuations in the next 5 minutes, and 284 samples are obtained, of which the first 3/4 are used as training samples, and the rest are used as test samples for model testing. The environment for the experiment is chosen from Matrix Lab (MATLAB). The study first compares the distribution of its original shrinkage and porosity characteristics with the distribution after FIG, and the results are shown in Figure 6.

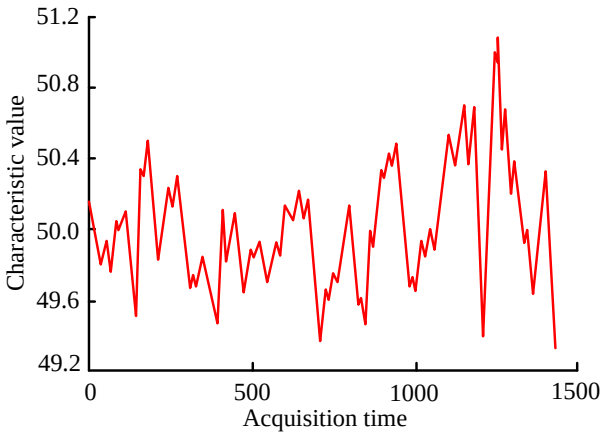

(a) Distribution of original condensation and porosity characteristics

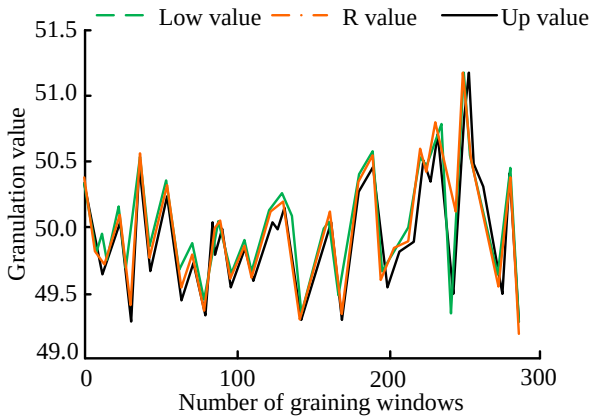

(b) Characteristic Distribution of Granulated Fuzzy Information

Figure 6: Comparison results of original characteristic distribution and distribution after FIG

From Figure 6(a), within the 1500s of collection, the shrinkage and bulk intrinsic viscosity of cotton and linen fabrics are in a state of violent fluctuation, and the values are maintained between 49.2-51.2. Among them, within 1000-1500s, the maximum and minimum values are reached, which are 51.15 and 49.3, respectively. From Figure 6(b) that after it is processed by FIG, the values of the three sequences are maintained on one line, and the values are roughly between 49.25-51.25. To sum up, the FIG-processed data are roughly kept on the original data line, which meets the requirements of the experiment. On this basis, the study takes the Low, R and Up series as examples, and uses the FIG-PSO-ELM method to predict them. The prediction results are shown in Figure 7.

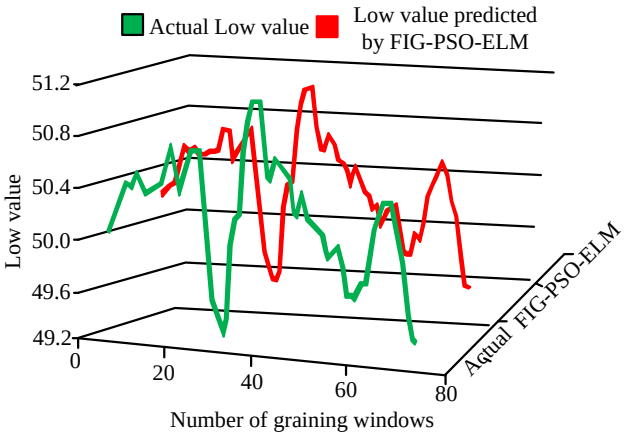

(a) Comparison Results of Low Series Real Value and Predicted Value

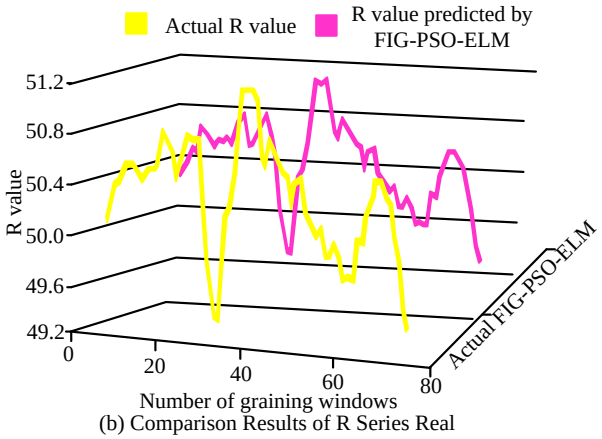

(b) Comparison Results of R Series Real Value and Predicted Value

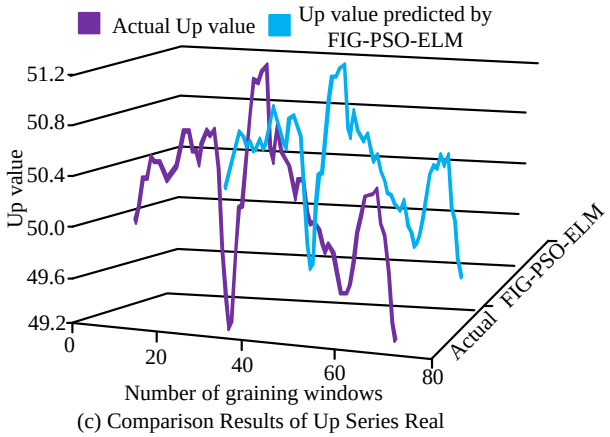

(c) Comparison Results of Up Series Real Value and Predicted Value

Figure 7: FIG-PSO-ELM prediction results on three sequences

Figures 7(a)~7(c) are the comparison results of the predicted value and the real value of the Low sequence, R sequence, and Up sequence, respectively. From Figure 7(a), when the granularity window is between 0-20, there is a discrepancy between the actual Low value and the Low predicted by FIG-PSO-ELM, which is maintained between 50.05-50.6. When the granularity window is between 20-70, the Low of the two is the same, maintained between 49.35-50.95, and the maximum value appears when the granularity window is between 30-40, which is 50.95. From Figure 7(b), the predicted R-value obtained by using FIG-PSO-ELM is consistent with the actual R-value, and the value is maintained between 49.4-51.0. Among them, the maximum value also appears in the grain window of 30-40, which is 51.0. From Figure 7(c), the actual Up value is consistent with the predicted value. The maximum still occurs in the graining window of 30-40 at 51.15. On the whole, the prediction results of the FIG-PSO-ELM selected in the study on the three sequences are consistent with the actual results, showing a high accuracy rate and strong effectiveness.

To further test the accuracy of the FIG-PSO-ELM, the study introduces Back-Propagation Neural Network (BPNN) and Radial Basis Function Neural Network (RBFNN). At the same time, PSO-ELM and traditional ELM models are selected, and the prediction results of the four algorithm models and the FIG-PSO-ELM model on the three sequences are compared. The results are shown in Figure 8.

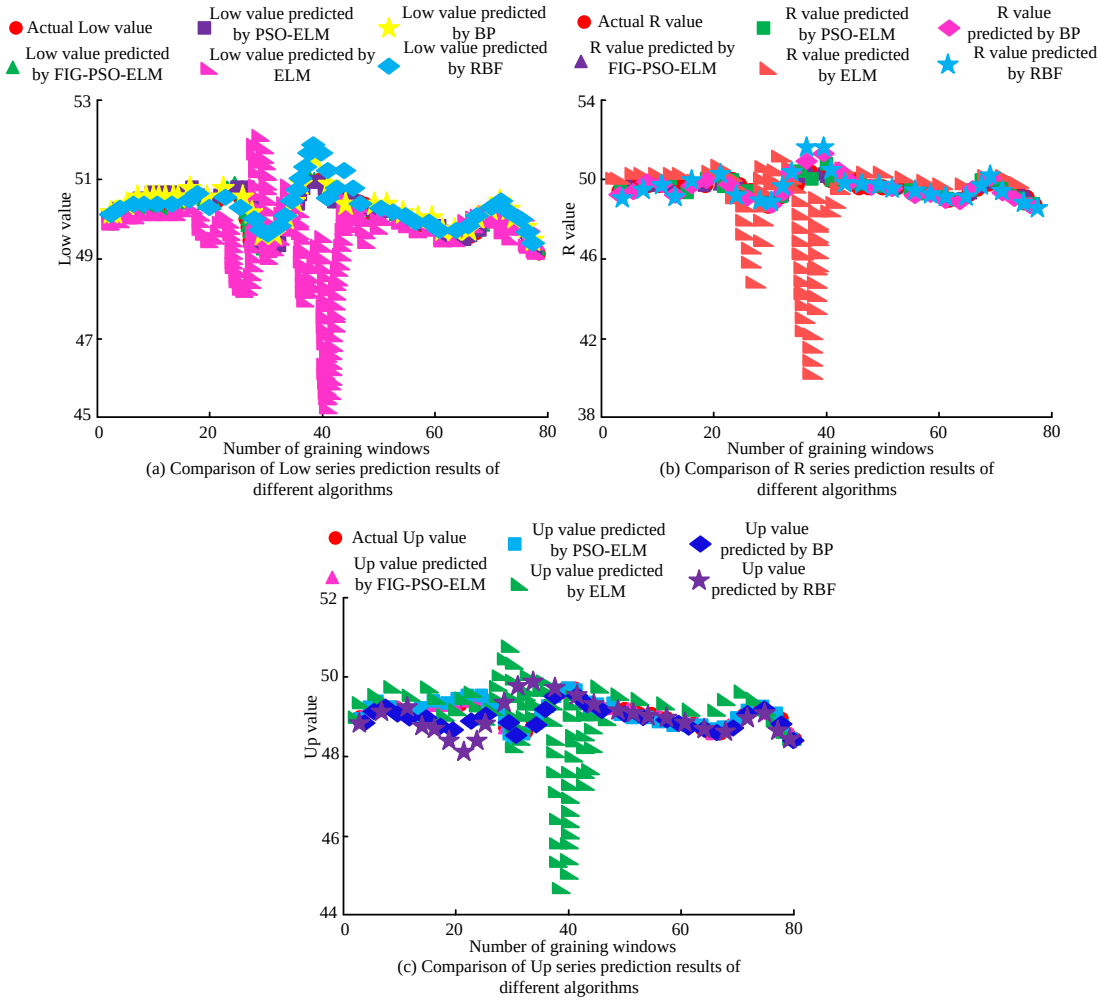

Figure 8: Prediction results of five algorithms on three sequences

From Figure 8, the predicted results of FIG-PSO-ELM are consistent with the actual results, and the values of the three are roughly maintained between 49 and 51. However, other algorithms will always have some differences under different granulation windows, especially the traditional ELM algorithm, which has obvious fluctuations, and the predicted results are quite different from the actual results. When the number of granulation windows is 20-40, there is an obvious gap. The minimum values of Low, R, and Up sequences are 45.1, 39.5, and 44.2, respectively, which show a poor fitting effect. On the whole, the performance effect of ELM is the worst, BPNN reduces the error due to the additional back-propagation process, and PSO-ELM uses

the PSO algorithm to optimize the parameters of ELM, thus avoiding the problem of decreasing prediction accuracy. The proposed FIG-PSO-ELM algorithm shows the highest prediction accuracy. In this process, after comparing the predicted values of the five algorithm models with the actual values, the corresponding *MSE* values and *MAE* values are obtained. The study compares the two error values between different prediction models, and the results are shown in Figure 9.

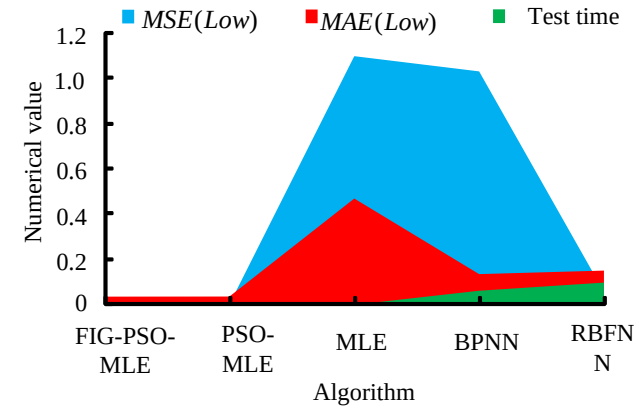

(a) Error Comparison Results of Five Algorithms on Low Sequence

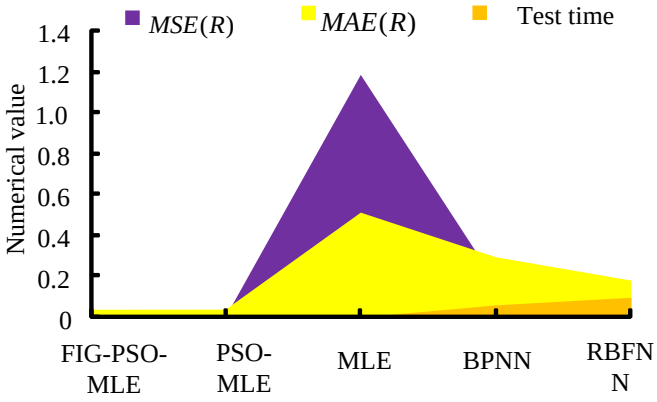

(b) Error Comparison Results of Five Algorithms on R Sequence

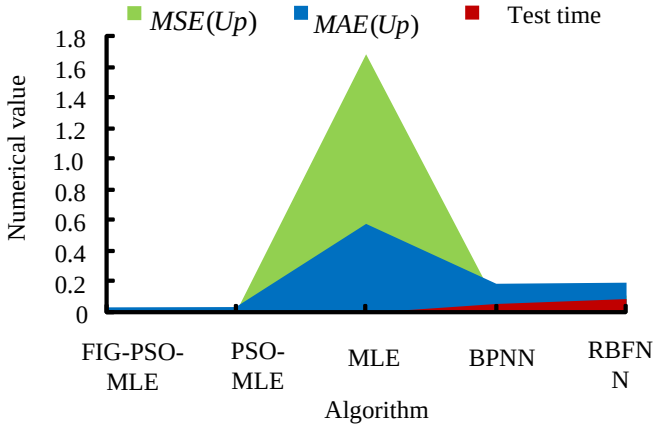

(c) Error Comparison Results of Five Algorithms on Up Sequence

Figure 9: Error comparison results of five algorithms on three sequences

From Figure 9, in the comparison of Low sequence errors, the *MSE* and *MAE* values of the FIG-PSO-ELM are the lowest, which are 0.0027 and 0.0369, respectively. The two error values of ELM are higher than other algorithms, and the highest *MSE* value reaches 1.1017. In the R sequence, the lowest *MSE* and *MAE* values of FIG-PSO-ELM are 0.0019 and 0.0387 respectively, and they are still far lower than 1.1861 and 0.5115 of the ELM algorithms models when the test time is higher than 0.0007s of ELM. Likewise, both errors of FIG-PSO-ELM are the lowest in the Up sequence. In general, the FIG-PSO-ELM model has good stability, and its prediction error remains unchanged for different sequence components; The stability of the PSO-ELM algorithm model is also good, and the prediction error is slightly higher than that of FIG-PSO-ELM. In terms of test time, the time spent by FIG-PSO-ELM is shorter than that of ELM. Therefore, the use of the FIG-PSO-ELM method can accurately predict the fluctuation range of shrinkage and porosity of cotton and linen fabrics, so that it can effectively improve its wrinkle resistance and reduce its surface roughness in weaving. Finally, the FIG-PSO-ELM algorithm is used to predict the polycondensation performance and porosity of various fabric types, namely cotton, linen, cotton-linen blend, silk and wool, to verify the generalization ability and accuracy of the algorithm. The experimental results are shown in Figure 10.

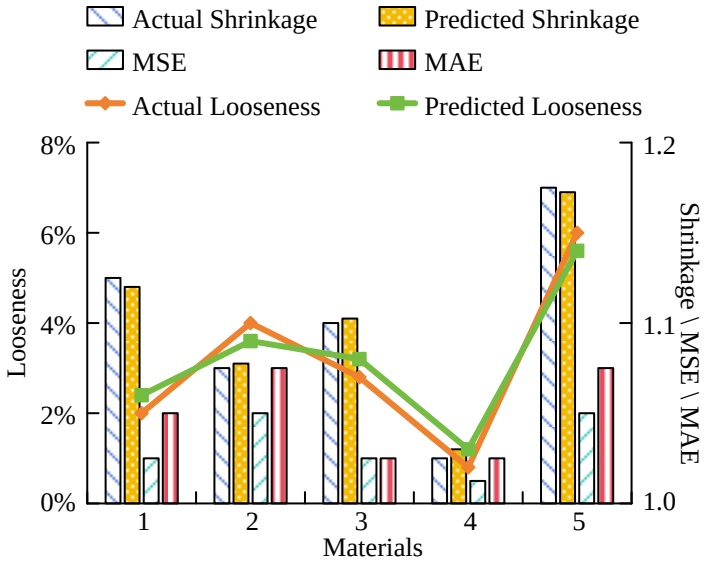

Figure 10: Experimental results

In Figure 10, the horizontal coordinates 1-5 represent cotton, hemp, cotton-hemp blend, silk, and wool, respectively. The FIG-PSO-ELM model performs well in predicting the shrinkage performance and porosity of different fabric types, with low *MSE* and *MAE*, indicating that the model can provide accurate predictions. Cotton and silk fabrics have the highest accuracy, while wool fabrics have relatively large errors, indicating that special optimization of the model may be required for some special fabric characteristics. In summary, the study not only proves the generalization ability of FIG-PSO-ELM algorithm, but also provides a practical forecasting tool for the textile industry in fabric quality control and production efficiency improvement.

5 Conclusion

To achieve effective control in the production of cotton and linen fabrics, and to improve their polycondensation performance and porosity, the PSO algorithm was used to optimize the ELM, and FIG was selected to extract the polycondensation and porosity characteristics of cotton and linen fabrics. The FIG-PSO-ELM algorithm was proposed and its effectiveness was verified. The results showed that within the 1500s of the collection, the intrinsic viscosity of cotton and linen fabrics fluctuated greatly, and the value was roughly maintained between 49.2-51.2. When the time was 1000-1500s, it reached the maximum (51.15) and minimum (49.3) value. In addition, on the Low, R, and Up sequences, the values predicted by the FIG-PSO-ELM were roughly the same as the actual values, maintaining between 49-51, showing high accuracy. At the same time, comparing with the predictive results of the other four algorithms on the three sequences, it was found that the FIG-PSO-ELM had the highest degree of agreement between the predictive results and the actual results. The ELM was the lowest, and the R sequence value reached a maximum of 39.5. On this basis, the study compared the sum of the five algorithms in *MSE* and *MAE*. It was found that the values of the FIG-PSO-ELM on the three sequences were significantly lower than those of the other four algorithms, with the lowest *MSE* value being 0.0019 and the *MAE* lowest value being 0.0368. In a word, the

FIG-PSO-ELM algorithm presented in the study shows high performance, which can accurately predict the fluctuation range of shrinkage and porosity of cotton and linen fabrics, and has a good effect on improving the quality of cotton and linen fabrics. However, the study only explores part of the content of the prediction model, which can be further explored in the subsequent defect detection.

Although the FIG-PSO-ELM algorithm has shown remarkable results in predicting the shrinkage performance and porosity of cotton and linen fabrics, future work can further expand its application and improve its performance. Specifically, a fault detection mechanism can be integrated to identify production anomalies in real-time, and the algorithm's generalization ability under different structures and conditions can be tested. Moreover, the efficiency of the algorithm can be optimized to handle real-time data streams, and a user-friendly interface can be developed to enhance the interaction experience. In addition, conducting long-term performance evaluations, fusing multi-modal data to improve the depth of predictions, improving the interpretability of algorithms, and promoting interdisciplinary collaboration are all potential directions to advance the field. Through these improvements, the FIG-PSO-ELM algorithm is expected to achieve a wider application in the textile industry and provide higher value.

6 Discussion

The proposed FIG-PSO-ELM method shows excellent performance in predicting polycondensation properties and porosity of cotton and linen fabrics. In previous studies, as described in reference [8], [9], and [10], enzymatic methods, continuous pad dyeing techniques, and the application of novel N-phenylmaleimide were all aimed at improving specific properties of wool fabrics. However, these methods mainly focused on specific fabric handling techniques without involving the use of data-driven models for performance prediction. In contrast, the FIG-PSO-ELM method uses advanced data-driven technology to dynamically predict fabric characteristics, which has significant advantages in real-time monitoring and production adjustment. The performance advantage of the FIG-PSO-ELM method can be attributed to several key factors. First of all, the improvement of the algorithm, especially the optimization of ELM by the PSO algorithm, improves the prediction accuracy and generalization ability of the model. Secondly, the application of FIG technology enhances the processing power of dynamic data, enabling the model to more accurately capture fluctuations in fabric characteristics. In addition, compared with traditional ELM and other neural network models, FIG-PSO-ELM is more efficient in data processing, as reflected in the experimental results, and its prediction error is significantly lower than other methods.

The FIG-PSO-ELM method has brought new contributions to the textile field. Its superior prediction accuracy and efficiency make it have important application value in the quality control of cotton and linen fabric production. This method can not only reduce the number of unqualified products but also improve production efficiency and reduce costs. In addition, the application of the FIG-PSO-ELM method can be extended to other types of fabrics and textile materials, providing new possibilities for the intelligence and automation of the textile industry.

Funding

The research is supported by: School-level scientific research and innovation platform project: collaborative innovation center for structural innovation and functional research and development of shoes and clothing product (No. PT21003/0301); Fujian Young and Middle-aged Project: Research on Friction Comfort of New Clothing Fabrics Based on Long-distance Running (No. JZ180909).

References

[1] B. K. Behera, “Comfort and handle the behavior of linen-blended fabrics,” AUTEX Research Journal, vol. 7, no. 1, pp. 33-47, 2007. https://doi.org/10.1515/aut-2007-070104

[2] M. Peng, C. Liu, S. Chen, S. Gao, L. Jiang, and J. Ma, “Development and performance study of a new shrink-proof and non-iron cotton blended fabric,” Textile Research Journal, vol. 89, no. 16, pp. 3269-3279, 2019. https://doi.org/10.1177/0040517518809043

[3] C. Saricam, “The comfort properties of hemp and flax blended denim fabrics with common industrial washing treatments,” Textile Research Journal, vol. 92, no. 17-18, pp. 3164-3178, 2022. https://doi.org/10.1177/00405175211054216

[4] T. Nongnual, S. Kaewpirom, N. Damnong, S. Srimongkol, and T. Benjalersyarnon, “A simple and precise estimation of water sliding angle by monitoring image brightness: A case study of the fluid repellency of commercial face masks,” ACS Omega, vol. 7, no. 15, pp. 13178-13188, 2022. https://doi.org/10.1021/acsomega.2c00628

[5] D. T. Birkocak, “Effects of needle size and sewing thread on seam quality of traditional fabrics,” Textile and Apparel, vol. 32, no. 3, pp. 277-287. https://doi.org/10.32710/tekstilvekonfeksiyon.1088043

[6] D. Atalie, and G. Ashagre, “Abrasion, pilling, and snagging properties of half-bleached bedsheet fabrics made from 100% cotton yarns with various parameters,” Journal of Natural Fibers, vol. 19, no.

10, pp. 3788-3796, 2022. https://doi.org/10.1080/15440478.2020.1848727

[7] N. Senthil, and B. Dhurai, "Knittability enhancement study of 100% linen yarn using softeners," Journal of Natural Fibers, vol. 19, no. 12, pp. 4393-4402, 2022. https://doi.org/10.1080/15440478.2020.1863287

[8] N. Zhang, P. Huang, P. Wang, Y. Yu, M. Zhou, and Q. Wang, "Combined cutinase and keratinolytic enzyme to endow improved shrink-resistance to wool fabric," Fibers and Polymers, vol. 23, no. 4, pp. 985-992, 2022. https://doi.org/10.1007/s12221-022-4445-0

[9] Y. Luo, S. Zhai, L. Pei, J. Wang, and Z. Cai, "Environment-friendly high-efficiency continuous pad dyeing of non-shrinkable wool fabric by the silicon fixation method without auxiliary chemicals," ACS Sustainable Chemistry & Engineering, vol. 10, no. 11, pp. 3557-3566, 2022. https://doi.org/10.1021/acssuschemeng.1c07793

[10] G. Liu, W. Wang, and D. Yu, "Facile fabrication of durable antibacterial and anti-felting wool fabrics with enhanced comfort via novel N-phenylmaleimide finishing," Bioprocess and Biosystems Engineering, vol. 45, no. 5, pp. 921-929, 2022. https://doi.org/10.1007/s00449-022-02710-2

[11] B. Šaravanja, S. Kovačević, T. Pušić, K. Malarić, and D. Ujević, "Impact of dry and wet cleaning on structural, mechanical and protective properties of fabrics designed for electromagnetic shield application," Fibers and Polymers, vol. 23, no. 3, pp. 666-679, 2022. https://doi.org/10.1007/s12221-022-3028-4

[12] B. Qi, F. Wang, Q. Chen, B. Xu, P. Wang, M. Zhou, and Q. Wang, "Enzymatic construction of a temperature-regulating fabric with multiple heat-transfer capabilities," Cellulose, vol. 29, no. 6, pp. 3513- 3528, 2022. https://doi.org/10.1007/s10570-022-04467-z

[13] V. Z. Fahritdinovna, T. S. Erkaevich, and P. O. Viktorovna, "Comparative analysis of the qualitative characteristics of national fabrics," Academicia Globe: Inderscience Research, vol. 3, no. 04, pp. 596-602, 2022. https://doi.org/10.17605/OSF.IO/8JGPN

[14] H. Zhang, Y. Cao, Q. Zhen, J. Cui, and X. M. Qian, "Facile preparation of PET/PA6 bicomponent microfilament fabrics with tunable porosity for comfortable medical protective clothing," ACS Applied Bio Materials, vol. 5, no. 7, pp. 3509-3518, 2022. https://doi.org/10.1021/acsabm.2c00447

[15] A. Fouda, P. Těšinová, A. Khalil, and M. Eldeeba, "Thermo-physiological properties of polyester chenille single Jersey knitted fabrics," Alexandria Engineering Journal, vol. 61, no. 9, pp. 7029-7036, 2022. https://doi.org/10.1016/j.aej.2021.12.041

[16] N. Dehghan, P. Payvandy, and S. Talebi, "Introducing a novel model for predicting effective thermal conductivity of spacer fabrics based on their structural parameters," Journal of Thermal Analysis and Calorimetry, vol. 147, no. 12, pp. 6615-6629, 2022. https://doi.org/10.1007/s10973-021-11000-0

[17] Y. E. Kim, Y. J. Bae, Y. S. Seok, and I. C. Um, "Effect of hot press time on the structure characteristics and mechanical properties of silk non-woven fabric," International Journal of Industrial Entomology, vol. 44, no. 1, pp. 12-20, 2022. https://doi.org/10.7852/ijie.2022.44.1.12

[18] S. J. Kim, and I. C. Um, "Preparation, structural characterization, and properties of natural silk non-woven fabrics from different silkworm varieties," Fibers and Polymers, vol. 23, no. 4, pp. 1130-1141, 2022. https://doi.org/10.1007/s12221-022-4350-6

[19] Z. Zhou, W. Deng, Y. Wang, and Z. Zhu, "Classification of clothing images based on a parallel convolutional neural network and random vector functional link optimized by the grasshopper optimization algorithm," Textile Research Journal, vol. 92, no. 9-10, pp. 1415-1428, 2022. https://doi.org/10.1177/00405175211059207

[20] P. Cheng, J. Wang, X. Zeng, P. Bruniaux, and X. Tao, "Motion comfort analysis of tight-fitting sportswear from multi-dimensions using intelligence systems," Textile Research Journal, vol. 92, no. 11-12, pp. 1843-1866, 2022. https://doi.org/10.1177/00405175211070611

[21] F. Shi, M. Wang, K. Fang, Z. Zhao, H. Zhao, and W. Chen, "Fabrication of chitosan-loaded multifunctional wool fabric for reactive dye digital inkjet printing by Schiff base reaction," Langmuir, vol. 38, no. 33, pp. 10081 -10088, 2022. https://doi.org/10.1021/acs.langmuir.2c00961

[22] H. Yildirim, and F. Ozturk, "A benchmark study of the material models for forming simulation of woven fabrics," The Journal of the Textile Institute, vol. 113, no. 6, pp. 1027-1038, 2022. https://doi.org/10.1080/00405000.2021.1914409